

Highly efficient luminescence from a hybrid state found in strongly quantum confined PbS nanocrystals

Mark J Fernée¹, Elizabeth Thomsen, Peter Jensen and Halina Rubinsztein-Dunlop

Centre for Quantum Computer Technology, School of Physical Sciences,
The University of Queensland, Queensland, 4072, Australia

E-mail: fernee@physics.uq.edu.au

Received 18 October 2005

Published 30 January 2006

Online at stacks.iop.org/Nano/17/956

Abstract

We report that high quality PbS nanocrystals, synthesized in the strong quantum confinement regime, have quantum yields as high as 70% at room temperature. We use a combination of modelling and photoluminescence up-conversion to show that we obtain a nearly monodisperse size distribution. Nevertheless, the emission displays a large nonresonant Stokes shift. The magnitude of the Stokes shift is found to be directly proportional to the degree of quantum confinement, from which we establish that the emission results from the recombination of one quantum confined charge carrier with one localized or surface-trapped charge carrier. Furthermore, the surface state energy is found to lie outside the bulk bandgap so that surface-related emission only commences for strongly quantum confined nanocrystals, thus highlighting a regime where improved surface passivation becomes necessary.

(Some figures in this article are in colour only in the electronic version)

1. Introduction

The development of high quality semiconductor nanocrystals (NCs) has led to the development of a wide range of new robust fluorescent materials that emit from the near ultraviolet to the mid-infrared. Many of these fluorophores are now available commercially². The physical properties of these nanomaterials depend sensitively on their size [1] and shape [2, 3] as well as composition. Therefore, the development of new types of NC can lead to new applications, based upon the unique properties of the material.

One such group of materials that possess potentially unique material properties are the lead chalcogenide semiconductors (or lead salts) [4]. These are a group of narrow band semiconductors possessing a simple and highly symmet-

ric crystal structure and hence a rather simple symmetric band-structure. They also exhibit exceedingly large exciton Bohr radii. Therefore, quantum confinement effects should be quite pronounced in these materials [4]. There has been a significant interest in these materials as infra-red fluorophores following the report of Murray *et al* [5] of a size tunable synthesis for high quality PbSe NCs. Room temperature quantum yields as high as 80% [6, 7] have been reported. Consequently, there has been a resurgence in interest of lead chalcogenide NCs. This includes reports on water soluble PbSe NCs for biological applications [8], highly stable PbSe/PbS core/shell NCs [9, 10], the use of PbSe NCs [11] and PbS NCs [12] as the active element in infrared organic LEDs, and of amplified spontaneous emission from closely packed PbSe NC superlattices [13], suggesting their use as tunable infrared lasers. Both PbS and PbSe NCs have also been shown to efficiently generate multi-exciton states via impact ionization [14, 15], which has great potential for improving the efficiency in photovoltaic applications. PbS and PbSe NCs are also available commercially (see footnote 2).

¹ Author to whom any correspondence should be addressed.

² Commercial suppliers of nanocrystals (such as Evident technologies and the Quantum Dot corporation) now sell a range of nanocrystals, including CdSe, CdSe/ZnS, CdTe/CdS, PbSe and PbS NCs, that span the visible and near infrared spectrum.

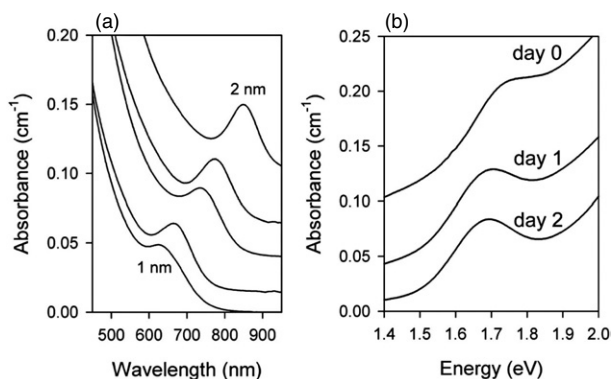


Figure 1. (a) Absorption spectra from a range of PbS NC solutions demonstrating that tuning of the first exciton peak throughout the strong quantum confinement regime can be achieved. (b) Natural size focusing of a PbS NC solution in hexane when stored in the dark at room temperature for two days. An absolute absorbance scale is used for direct comparison, revealing the dramatic reduction in the infrared tail that occurs with the size focusing.

The quality of a fluorophore is often indicated by its quantum yield. A high quantum yield is usually associated with NCs having well passivated surfaces, allowing efficient recombination of the delocalized intrinsic semiconductor states. However, recently it was reported that for CdSe NCs charge-carrier recombination involving one charge carrier trapped in a surface state can also have high luminescence quantum yields [16]. That report highlighted the fact that high quality emission need not necessarily emanate from pure intrinsic exciton recombination. For lead salt NCs in the strong quantum confinement regime, proper surface passivation should be extremely important, as both charge carriers should strongly interact with the surface due to the quantum confinement. This is of great concern for organically passivated surfaces, as only one surface species is usually passivated [17]. Here, we report that oleic acid capped PbS NCs synthesized in the strong quantum confinement regime have quantum yields as high as 70% at room temperature. However, the emission is strongly Stokes shifted. Using the Stokes shift data, we provide evidence that the emission results from the recombination of one quantum confined charge carrier with one localized or trapped charge carrier. We are able to identify the quantum confinement regime where this effect becomes important, thus highlighting a regime where improved surface passivation becomes necessary.

2. Experimental methods

PbS NCs are synthesized according to a slight variant of the procedure that was developed for producing NCs in the strong quantum confinement regime [18]. This procedure was based on that described by Hines and Scholes [19] for producing the smallest PbS NCs, although a different non-coordinating solvent (n-decane) and sulfur source (H₂S gas) are used. The synthesis procedure is described in detail in appendix A. The as-prepared solutions were stored in the dark for two days to a week, which allows a form of digestive ripening and line narrowing to occur [19] (see figure 1(b)).

Absorption measurements were made using a Perkin Elmer Lambda 40 UV/vis absorption spectrometer. Luminescence measurements were made using 532 nm excitation from a frequency doubled CW YAG laser and detected at 90° to the excitation beam using a 300 mm single-grating spectrometer (Acton) equipped with a silicon photodiode. PLE and other luminescence measurements were conducted using a fluorescence spectrometer (Spex Fluoromax 3) equipped with a Hamamatsu R928 photomultiplier tube. Appropriate background subtraction and detector response calibrations were included.

3. Results and discussion

PbS NC solutions displaying a progression of first exciton peaks from 1000 nm in the near infrared to less than 600 nm in the visible [18] are possible using the synthesis we employed for this study. The range of PbS NCs that is possible with this synthesis is useful in that it provides NCs with a tunable excitonic absorption peak in a strongly quantum confined region that was not covered by other existing syntheses. In particular, it bridges the gap between the strongly quantum confined PbS NCs obtained using a long-standing aqueous procedure [23] (and other variants [24, 25]) and the more widely acknowledged size tunable syntheses based on various glasses [26] and the recently developed organic synthesis of Hines and Scholes [19]. The progression in absorption spectra that can be obtained is illustrated in figure 1(a). The natural size focusing that was used to eliminate the infra-red tail and narrow the initial size distribution is shown in figure 1(b). While Hines and Scholes discuss this remarkable phenomenon at length [19], our data show that the size focusing can also increase the mean size of the distribution. Nevertheless, the mono-disperse sub-ensemble feeds off the significant poly-disperse ensemble of larger NCs, in a process opposite to the well known process of Ostwald ripening.

This range of exciton peak energies has been shown to correspond to particles with sizes ranging from approximately 1 to 2 nm in diameter [18]. With the addition of the work of Hines and Scholes [19], there now exists a continuous tuning range for PbS NCs with band-edge excitonic peaks ranging from 580 to 1800 nm, corresponding to sizes ranging from 1 to 8 nm respectively. The continuity in the evolution of the excitonic peak with particle size suggests that quantum size effects are prevalent across the entire tuning range, while molecular cluster-like behaviour is not apparent (for example, there are no apparent ‘magic’ sizes/shapes). On the other hand, in this strong quantum confinement regime, there may be a continuous variation in NC stoichiometry away from that of the bulk semiconductor, as hinted at by the change in the ratio of reactants required to form the smallest NCs. Thus referring to these NCs as PbS may be slightly misleading if there is a changing stoichiometry. We speculate that a variation in stoichiometry may be driven by the surface capping ligands that bind to only one of the two atomic species [17]. It may well be that similarly sized PbS NCs with different stoichiometries can have dramatically different optical properties, which could explain some rather anomalous results obtained for PbS NCs in the past [23–25, 27].

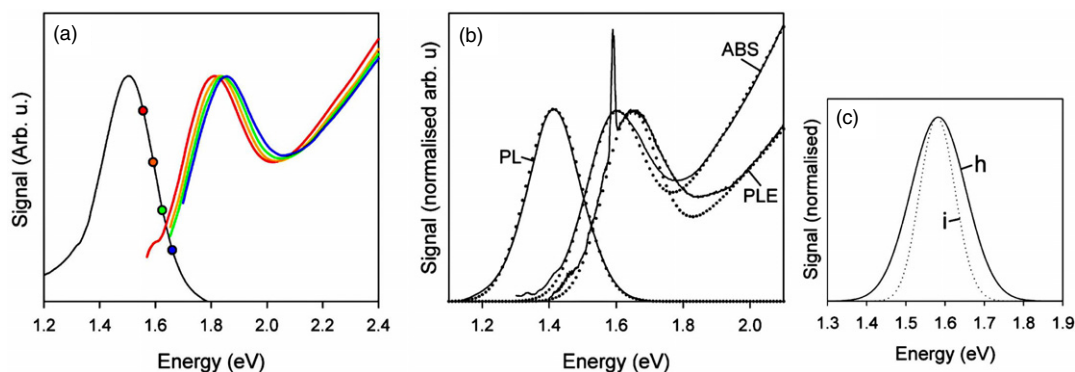


Figure 2. (a) PL and associated PLE spectra for a PbS NC solution in hexane. The PLE spectra were obtained using a 3 nm band-pass and monitoring the emission at 800, 780, 760 and 740 nm (filled circles). (b) Absorption, PL and PLE spectra for a single PbS NC solution in hexane are shown (lines). The sharp peak in the PLE spectrum indicates the detection energy. Dotted lines represent the model curves obtained from simulations of the absorption, PL and PLE processes based on a size distributed ensemble of single-nanocrystal spectra. (c) The homogeneous (solid curve—h) and inhomogeneous (dotted curve—i, due to size dispersion) contributions to the excitonic peak in (b) as determined by the model fit to the three spectra.

The PbS NCs in the size range between 1 and 2 nm are no longer adequately described by theoretical models such as those developed by Kang and Wise [28]. Instead of resorting to more elaborate models that include band-structure complexities away from the bandgap region, it has been suggested that an adequate model based on charge-carrier effective masses can be constructed if a finite confinement potential is included [29]. Models that include a finite confinement potential have proven much more successful in predicting the lowest exciton energy as a function of particle size for various NC materials in the strong quantum confinement regime [29]. We also find that the finite confinement barrier PbS NC model more adequately describes our observations. The continuous tuning of the excitonic peak that can be obtained with the synthesis used in this study suggests that such a model may still be valid, even for NCs as small as 1 nm [18]. However, the consequences of partial confinement of the exciton wavefunction due to a finite potential have not yet been addressed. Therefore, the synthesis of stable PbS NCs in this strong quantum confinement regime provides an opportunity to test this theory.

We perform a series of absorption, photoluminescence (PL) and photoluminescence excitation (PLE) scans in order to investigate the quality of the strongly quantum confined PbS NCs used in this study. It is well known that PLE spectroscopy is size selective [30] and as such is a useful means of investigating the size dispersion of a sample. In figure 2(a) a series of PLE curves are plotted along with the PL spectrum of a solution of PbS NCs in hexane. The PLE curves are normalized to the same excitonic peak height to illustrate that minimal peak shift accompanies large shifts in the monitoring energies (indicated on the PL curve). We also see that the PLE linewidths are comparable to the PL linewidth. These properties are characteristic of high quality emission that is predominantly homogeneously broadened. In figure 2(b) we plot the absorption, PL and PLE spectra of another PbS NC solution. The data are plotted on a normalized scale so that the exciton peaks coincide. We see a well defined excitonic peak in absorption, which is generally indicative of a high quality synthesis. The photoluminescence (PL) lineshape is virtually

identical to the excitonic absorption lineshape, suggesting emission from a single quantum state. The PLE curve monitors emission on the far blue edge of the PL spectrum near the absorption peak maximum. It also has a similar excitonic peak with a full width at half maximum (FWHM) identical to the absorption peak. By monitoring the extreme blue edge of the emission for the PLE spectrum, we are employing size selective spectroscopy, which should yield information about the smallest NCs in the size distribution of the solution. This is manifest in the peak shift of the PLE spectrum relative to the absorption spectrum (40 meV). However, this shift is considerably smaller than the emission offset relative to the PL peak position (180 meV). This suggests that the size distribution is not the dominant factor determining the FWHM of the excitonic feature. Furthermore, contributions to the PLE lineshape contain a component of up-converted emission (indicated by energies below the sharp spike on the spectrum). The fact that the up-converted portion of the PLE curve provides no noticeable distortion of the excitonic peak lineshape, thus representing linear absorption beyond 200 meV below the emission energy, indicates that the PLE excitonic peak is predominantly homogeneously broadened. A large non-resonant Stokes shift is evident in both figures 2(a) (approximately 300 meV) and 2(b) (approximately 200 meV).

A simple model was employed in order to model the signals that were collected in figure 2(b) and gain further insight into the lineshape contributions and the non-resonant Stokes shift. The model is based on an assumed single NC absorption and emission spectrum consisting of an excitonic lineshape curve with the addition of a non-linear rising background term for the absorption spectrum. A Gaussian distribution of sizes was then employed, in conjunction with the PbS NC quantum confinement model of Marin *et al* [29] in order to determine the distribution of single NC spectra to be used to model the system. Effects of size selective pumping, re-absorption of the emission and size-biased absorption were naturally included. The output of the model is shown as dotted lines in figure 2(b). Excellent fits to the excitonic features could only be obtained for a Gaussian single NC lineshape, and not a Lorentzian. By simultaneously fitting the spectral

widths and peak positions to the three spectra, an estimation of the energy dispersion due to the size distribution as well as the homogeneous contribution to the spectra could be obtained. Thus a large homogeneous linewidth of 165 meV was determined along with a smaller inhomogeneous linewidth of 110 meV, corresponding to a 8% size dispersion (figure 2(c)). The estimated size distribution corresponds to approximately a one monolayer thickness variation for 2 nm NCs, suggesting that surface roughness is responsible for the size distribution. The rather large homogeneous linewidth needs some comment. Initial low temperature studies show a significant narrowing of the lineshape with reducing temperature, validating the claim that inhomogeneous broadening does not dominate the lineshape. Nevertheless, the line narrowing is not consistent with pure phonon broadening of the homogeneous lineshape. However, it has been predicted that inter-valley scattering will split the eightfold degenerate ground state [31]. It is also expected that shape anisotropy will also contribute to the splitting of the degenerate ground state [13, 28, 30]. These effects should result in a lineshape composed of an ensemble distribution of four separate spin-degenerate states with shape-dependent separations. This is in accord with the observation by Hines and Scholes that PbS NCs size focus into non-spherical highly faceted shapes [19] along with the report by Hens *et al* that departures from spherical symmetry can strongly influence the energy structure of PbS NCs [3]. Importantly, this model could not account for the observed Stokes shift of the emission peak based on the inhomogeneous size distribution, so a Stokes shift parameter of 175 meV had to be included.

Another important property that is often used to determine the quality of an NC is its quantum yield. We determined the quantum yield of a number of samples using Rhodamine 101 and Rhodamine 6G as well known reference standards. The procedure required using carefully calibrated spectrometers due to the dye's emission in the visible region of the spectrum compared to the PbS NCs infrared emission. These standards were chosen because of the paucity of good quantum yield standards in the infrared. For example, the results obtained from the 2 nm PbS NCs used in figure 2(b) are shown in figure 3(a). A plot of absorbance versus integrated emission for both the Rhodamine 101 reference and the PbS NC solution is used. The slope of the reference data is directly proportional to the quantum yield (which has a known quantum yield of unity). This allows the determination of unknown quantum yields. We find the PbS NC data have two approximately linear regions, which allow a confident determination of the quantum yield in these regions. The quantum yield is approximately 40% for off-resonant excitation and up to 70% for resonant excitation of the excitonic peak. We tentatively attribute the lower value to the presence of a residual background of larger NCs forming a long infrared tail, which adds additional loss for non-resonant excitation. In figure 3(b) we use the non-resonant quantum yield to spot calibrate and scale a PLE curve against the absorption curve, using the fact that the PLE curve should be directly proportional to the product of the absorption and quantum yield. Thus the ratio of the absorption spectrum and PLE spectrum should also give an estimate of the spectral dependence of the quantum yield. Again we find a high resonant quantum yield compared to the

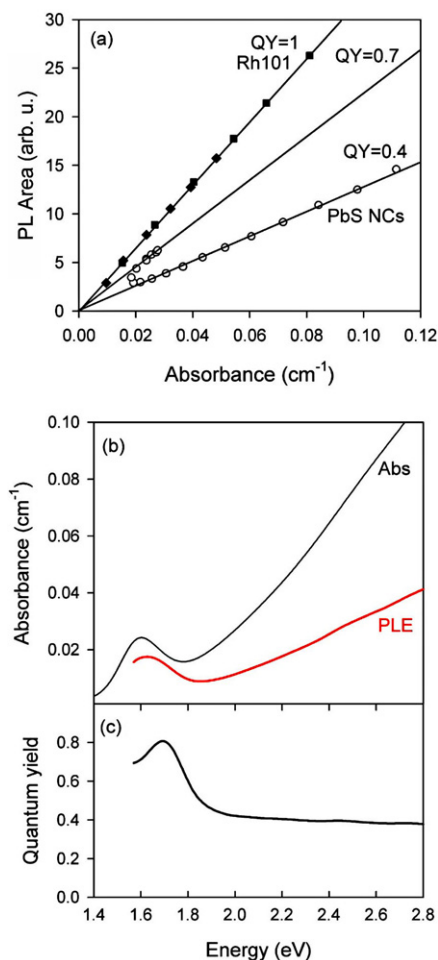


Figure 3. (a) A plot of integrated PL versus absorbance for Rhodamine 101 in basic ethanol (quantum yield standard) and a PbS NC solution in hexane (solution used in figure 2(b)). The data points for the reference dye were obtained using a series of six dilutions and two different pump wavelengths (solid diamonds and solid squares), while the data points for the PbS NC solution were obtained by pumping at different wavelengths. (b) The absorbance and PLE curves for the PbS NC solution, where the PLE has been normalized according to the quantum yield obtained when pumping at 532 nm and the absorbance at 532 nm. (c) The spectral dependence of the quantum yield obtained by dividing the normalized PLE spectrum by the absorption spectrum.

off-resonant one. Therefore, we can establish, with reasonable confidence, a quantum yield as high as 70% for these 2 nm NCs. The quantum yield was found to decrease to about 20% for the smaller NCs. These relatively large quantum yields are comparable to what has been found for oleic acid capped PbSe NCs [6, 7] and comparable to or greater than that reported by Hines and Scholes for oleic acid capped PbS NCs [19]. This attests to the quality of the PbS NCs produced in the strong quantum confinement regime.

The observation of a large Stokes shift of the emission for CdSe NCs has been well documented. In this case the phenomenon was carefully explained in terms of fine structure splitting due to the crystal field anisotropy, shape anisotropy and the exchange coupling interaction, with the concomitant generation of a dark state [32]. For PbSe NCs (and by close association, PbS) with their highly symmetric cubic crystal

lattices, the current best theories also predict excitonic fine structure splitting of the eightfold degenerate ground state, in this case arising from inter-valley scattering [31]. So this may in fact contribute to a Stokes shift in the same way as for CdSe NCs. However, no dark states are predicted within the PbS and PbSe NC lowest energy exciton fine structure [31], which would be expected to lessen the effect that fine structure splitting has on the non-resonant Stokes shift.

When considering the PbS NC absorption, PL and PLE spectra, we see that the emitting state appears to be inextricably related to the excitonic absorption peak. This suggests emission from some non-localized quantum confined state within the NC. Furthermore, the emission lifetime for the smallest PbS NCs (band edge at 580 nm) is extremely long at $1 \mu\text{s}$ [18]. Surprisingly long lifetimes have been also observed in PbSe NCs, which prompted Wehrenberg *et al* [7] to propose that a dielectric screening effect could be responsible. Other candidates that could be responsible for such long emission lifetimes are dark states (spin forbidden transitions [32]), indirect recombination (momentum forbidden transitions [33]) or charge separated states (such as a surface state [16] or a single trapped charge carrier). Both dark states and indirect transitions have not been predicted by the current lead salt NC theories [28, 31, 34, 35]. The case for dielectric screening was used for PbSe NCs, which have a larger bulk dielectric constant. We repeated the calculation with the appropriate dielectric constants for PbS and the solvent, hexane (noting that PbS has nearly the same oscillator strength as PbSe [28]). The lower dielectric constant for PbS suggests a reduction in the dielectric screening effect. We find that the PbS lifetimes should be as much as 50% shorter than those for PbSe NCs, quantum confinement effects on the dielectric function notwithstanding [36]. Therefore, dielectric screening may not be solely responsible for the long microsecond lifetimes that are observed.

Further insight into the luminescence character can be obtained through comparison with data from other reports of PbS NCs exhibiting similar degrees of quantum confinement. For PbS NCs synthesized in an ethanol solvent, a significantly smaller Stokes shift was found [25]. Also, a smaller Stokes shift (consistent with the results of the ethanol synthesized PbS NCs) was found from PbS NCs that were surface passivated using cadmium sulfide precursors [37]. This suggests that the Stokes shift in the emission is associated with the surface passivation of the PbS NCs (in contrast to the Stokes shift found in CdSe NCs [32]) and so could indicate the presence of a surface state [16] or surface trapping of one of the charge carriers.

The quantum confinement of only a single charge carrier is directly indicated when plotting the position of the PL peak as a function of the absorption excitonic peak position. Such a plot is shown in figure 4 and reveals a linear trend with increasing blue shift of the absorption excitonic peak. Such a linear relationship indicates that both emitting and absorbing states are *similarly* quantum confined (i.e. they share the same functional relationship with the size of the NC). However, the slope of the line is approximately 0.5, indicating that the rate of increase in quantum confinement is different for the excitonic absorbing state and the emitting state. For lead salts, which have charge carriers with nearly

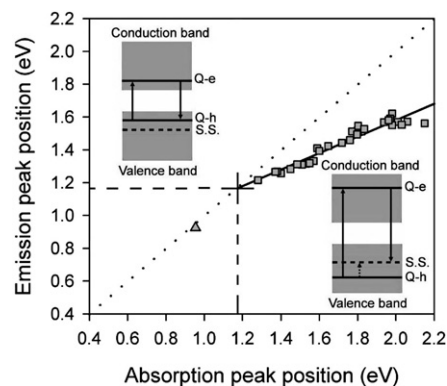


Figure 4. A plot of the emission peak position as a function of the position of the excitonic peak seen in the absorption spectrum for PbS NC synthesized in the strong quantum confinement regime (squares). The axes represent the entire tuning range of the PbS NC exciton peak, from the bulk band edge at 0.41–2.2 eV. A dotted line represents the zero-Stokes-shift line. All Stokes shifted emission should correspond to points below the line. A triangle represents the datum obtained from the work of Hines and Scholes [19]. A line of best fit is included for the strongly quantum confined data (solid). The slope of the line is 0.50 and the cross at the end of the line marks the crossing of the zero-Stokes-shift line at 1.16 eV. From these data we are able to establish the existence of a charge localizing or surface state (S.S.) that is most likely to lie at least 0.375 eV below the edge of the bulk PbS valence band. Non-Stokes shifted emission results when energy relaxation can proceed to the quantum confined lowest energy states (left inset). Stokes shifted emission results when there is sufficient quantum confinement energy so that the surface state becomes the lowest energy state for one of the charge carriers (right inset). We have located the surface state within the bulk valence band as a trap for holes (see text). Solid arrows are used to represent radiative processes (excitation, up arrow; recombination/emission, down arrow), while the dotted arrow represents non-radiative relaxation.

equal effective masses, the rate of change of exciton quantum confinement is approximately twice the rate of a change of the individual charge carriers. Therefore a slope of 0.5 is consistent with emission from a state comprising only one quantum confined charge carrier, indicating the presence of some localized state. As this state seems to be dependent on the details of the surface passivation, we will refer to it as a surface state. Extrapolation of the straight line fit readily indicates 1.16 eV (approximately 1070 nm) as the energy at which there should be zero Stokes shift according to this trend. We note that for an inhomogeneously broadened ensemble of NCs a Stokes shift should always be present due in part to phonon emission [32] and photon absorption being biased towards larger NCs. Therefore, a point on the line at 1.16 eV is not physically possible and the terminus of the linear trend would be found at a slightly greater energy. However, the important fact is that the linear trend terminates near the *middle* of the PbS NC size-tuning range (marked with a cross in figure 4), confirming the origin of the Stokes shift as due to a surface state and not an intrinsic state. We use this point to estimate a lower bound for the energy of the surface state as either 0.375 eV above the bulk semiconductor conduction band-edge, or 0.375 eV below the bulk semiconductor valence band-edge (based on a room temperature bulk bandgap of 0.41 eV).

The presence of a surface state in oleic acid passivated PbS NCs is not too surprising, as we know that oleic acid

only binds to the lead atoms at the surface [17]. This leaves the possibility of unpassivated sulfur atoms, which can act as shallow hole traps. Therefore, it is likely that the surface state is comprised of unpassivated sulfur atoms and lies more than 370 meV below the bulk semiconductor valence band-edge (see the insets of figure 4). The occupation of the surface state would then require sufficient quantum confinement of the holes so that the surface state becomes the lowest energy state accessible to the holes. This is the probably the reason why a significant Stokes shift in the emission was not mentioned in the initial report on oleic acid capped PbS NCs by Hines and Scholes [19], as most of their data are not sufficiently quantum confined to observe this effect. This is illustrated using a datum from their work in figure 4 (triangle), which we see clearly does not fit on the linear trend of our data.

Under these circumstances, we might not expect good isolation of the charge carriers as surface localized charge carriers have a far greater probability of interacting with the surrounding matrix. However, it has recently been shown that the presence of surface states does not necessarily lead to increased luminescence quenching [16]. Similarly, we found room temperature quantum yields as high as 70% when exciting at the excitonic absorption peak, which indicates that there is minimal luminescence quenching. Therefore, we also find highly efficient surface-related emission for strongly quantum confined PbS NCs.

The observed Stokes shift of the emission peak from the excitonic absorption peak can be far greater than both thermal energies at room temperature and phonon energies [38, 39], and therefore we would not expect efficient transport to take place. However, the evidence is to the contrary, as little or no emission attributable to recombination of the band-edge exciton is observed. From the work on PbSe NCs [6, 7] one can speculate that the radiative lifetime of the band-edge exciton in PbS NCs should be in the range of tens to hundreds of nanoseconds. Therefore, some form of efficient transport must be taking place between the excitonic absorbing state and the emitting state, so that the depopulation of the excitonic state proceeds at a rate considerably faster than the radiative lifetime. The discovery of a surface state in the PbS NC introduces the possibility that there may in fact be a manifold of surface states through which efficient energy relaxation can occur. The dramatic influence of such states on intra-band energy relaxation has recently been demonstrated in CdSe [40]. The existence of a manifold of surface states that interact with the intrinsic states of an NC could explain the efficient energy relaxation observed in oleic acid capped PbSe NCs and hence the absence of a phonon bottleneck [7].

4. Conclusions

We have reported that highly efficient emission in strongly quantum confined PbS NCs emanates from a hybrid state, comprising one quantum confined charge carrier and one surface-localized charge carrier. Quantum yields as high as 70% were found. The energy of the surface state was found to lie outside the bulk PbS bandgap region, so that hybrid state emission only occurs with sufficiently strong quantum confinement. This highlights a region of strong quantum confinement where improved surface passivation

becomes necessary if intrinsic charge-carrier dynamics are to be observed. For the strongly quantum confined PbS NCs, due to the fact that *both* charge carriers can be strongly quantum confined in lead salt NCs, the most effective means of surface passivation is likely to be epitaxial overcoating with a suitable wide bandgap semiconductor³. On the other hand, efficient surface trapping of a single charge carrier may be an effective means of charge separation for photovoltaic applications. Overall, our study clearly points to a critical confinement energy (for oleic acid capped PbS NCs) below which pure intrinsic exciton dynamics are possible.

Acknowledgments

We would like to thank J Warner for supplying some nanocrystal samples used in this study. All work was supported by the Australian Research Council.

Appendix A

In a typical synthesis, we used 0.1 g of lead acetate dissolved in a mixture of 0.4 ml of oleic acid and 4.6 ml of anhydrous n-decane. The molar ratio of lead cations to oleic acid molecules is 1:2 respectively. The lead precursor mixture is initially heated to 130 °C for 30 min, whilst being continuously stirred and purged with either argon or nitrogen, before being cooled to the required reaction temperature. The sulfur anions are introduced with an injection of 1 ml of H₂S at a rate of 0.1 ml s⁻¹. The molar ratio of sulfur ions to lead ions is 1:2 respectively. The reaction is allowed to proceed for 1 min and is then stopped by the rapid addition of a 20-fold excess of hexane and is stored in the refrigerator (usually 1 ml of the reaction mixture is removed and diluted in 18 ml of hexane). Size is controlled primarily through adjustment of the reaction temperature between 40 and 130 °C, with the lower temperature producing the smallest NCs. We have also found that the smallest NCs are more stable if synthesized with 0.8 ml of H₂S, corresponding to a lead to sulfur molar ratio of 5:2. The as-prepared solutions often have an infrared tail evident in the absorption, due to a poly-disperse ensemble of larger NCs. An extra size selective precipitation step can be employed to remove these larger NCs. However, a natural size focusing procedure was solely employed in this study. This involved nothing more than storing the solutions at room temperature in the dark for from two days to a week, which allows a form of digestive ripening and line narrowing to occur [19] (see figure 1(b)).

Appendix B

Quantum yields were determined relative to two well known reference dyes: rhodamine 101 in basic ethanol (Q.Y. = 1 [20]) and rhodamine 6G in ethanol (Q.Y. = 0.95 [21]).

A range of dye concentrations was used to provide an integrated intensity versus absorbance plot (as shown in figure 3(a)), the slope of the plots being directly proportional to the quantum yield. Two dyes were used in order to provide

³ Strontium sulfide is one such material that should be highly suited to the epitaxial overgrowth of lead salts.

a cross-calibration of the plot. We employed the following two-step procedure for determining quantum yields of the PbS NCs: luminescence spectra were obtained from both the reference dyes and PbS NCs using a calibrated fluorescence spectrometer (Spex, Fluoromax 3). This apparatus ensured that close to identical excitation and detection conditions could be met for both the reference dye and the PbS NCs. However, as the photomultiplier tube was operating at the end of its useful detection range for the PbS NC luminescence, the full spectral lineshape could not be obtained. Therefore, a second spectrometer equipped with a silicon photodiode was employed to detect the entire spectral lineshape. This spectrometer (including the entire detection path) was carefully calibrated using a tungsten standard lamp to ensure the accuracy of the lineshape. Multiple spectra were obtained over a range of pump laser powers to ensure that the lineshape was not power dependent. This then produced a known spectral lineshape for each particular PbS NC sample. This lineshape was then fit to the portion of the spectrum obtained with the photomultiplier and was used to provide the low energy tail of the spectrum, allowing the spectrum to be integrated in order to provide a datum on the integrated intensity versus absorbance plot. At least 30% of the spectrum was acquired by the fluorescence spectrometer in order to minimize errors with the procedure. For the PbS NCs, a range of absorbances was achieved by using different excitation energies. For an excitation-energy independent quantum yield this data would produce a linear trend, providing an accurate determination of the quantum yield. Otherwise, the data would provide a series of spot calibrations for the quantum yield at different excitation energies.

This procedure neglects any lineshape variation in the low-energy portion of the spectrum and so introduces some error in the quantum yield. Our estimate of this error, based on a study of the lineshape variation observed in the high energy portion of the spectrum, is in the vicinity of 10% and occurs primarily when exciting in the region of the excitonic peak (where the maximum amount of lineshape variation occurs [22]). This reasonably small error is also supported by the very small amount of spectral line narrowing obtained from PLE spectra such as in figure 2(a). Furthermore, a quantum yield determined for 532 nm excitation (thus avoiding any lineshape variation) was used to calibrate a PLE spectrum relative to the absorption spectrum, resulting in quantum yields consistent with that determined by the above procedure.

References

- [1] Murray C B, Norris D J and Bawendi M G 1993 *J. Am. Chem. Soc.* **115** 8706–15
- [2] Manna L, Scher E C and Alivisatos A P 2000 *J. Am. Chem. Soc.* **122** 12700–6
Peng X *et al* 2000 *Nature* **404** 59–61
- [3] Lee S, Jun Y, Cho S and Cheon J 2002 *J. Am. Chem. Soc.* **124** 11244–5
- [4] Hens Z, Vanmaekelbergh D, Stoffels E and van Kempen H 2002 *Phys. Rev. Lett.* **88** 236803
- [5] Wise F W 2000 *Acc. Chem. Res.* **33** 773
- [6] Murray C B *et al* 2001 *IBM J. Res. Dev.* **45** 47
- [7] Du H *et al* 2002 *Nano Lett.* **2** 1321
- [8] Wehrenberg B L, Wang C and Guyot-Sionnest P 2002 *J. Phys. Chem. B* **106** 10634
- [9] Yu W, Falkner J, Shih B and Colvin V 2004 *Chem. Mater.* **16** 3318
- [10] Sashchiuk A, Langof L, Chaim R and Lifshitz E 2002 *J. Cryst. Growth* **240** 431
- [11] Brumer M *et al* 2005 *Adv. Funct. Mater.* **15** 1111
- [12] Steckel J S, Coe-Sullivan S, Bulovic V and Bawendi M G 2003 *Adv. Mater.* **15** 1862
- [13] Bakueva L *et al* 2003 *Appl. Phys. Lett.* **82** 2895
- [14] Schaller R D, Petruska M A and Klimov V I 2003 *J. Phys. Chem. B* **107** 13765
- [15] Schaller R and Klimov V 2004 *Phys. Rev. Lett.* **92** 186601
- [16] Ellingson R *et al* 2005 *Nano Lett.* **5** 865
- [17] Wang X, Qu L, Zhang J, Peng X and Xiao M 2003 *Nano Lett.* **3** 1103
- [18] Lobo A *et al* 2005 *J. Phys. Chem. B* **109** 17422
- [19] Warner J H, Thomsen E, Watt A R, Heckenberg N R and Rubinsztein-Dunlop H 2005 *Nanotechnology* **16** 175–9
- [20] Hines M A and Scholes G D 2003 *Adv. Mater.* **15** 1844
- [21] Karstens T and Kobs K 1980 *J. Phys. Chem.* **84** 1871
- [22] Magde D, Wong R and Seybold P G 2002 *Photochem. Photobiol.* **75** 327
- [23] Hoheisel W, Colvin V L, Johnson C S and Alivisatos A P 1994 *J. Chem. Phys.* **101** 8455
- [24] Nenadovic M T, Comor M I, Vasic V and Micic O I 1990 *J. Phys. Chem.* **94** 6390
- [25] Gallardo S, Gutierrez M, Henglein A and Janata E 1989 *Ber. Bunsenges. Phys. Chem.* **93** 1080
- [26] Lu S, Sohling U, Krajewski T, Mennig M and Schmidt H 1998 *J. Mater. Sci. Lett.* **17** 2071
- [27] Kolobkova E V, Lipovskii A A, Petrikov V D and Melekhin V G 2002 *Glass Phys. Chem.* **28** 251
- [28] Machol J L, Wise F W, Patel R C and Tanner D B 1993 *Phys. Rev. B* **48** 2819
- [29] Kang I and Wise F W 1997 *J. Opt. Soc. Am. B* **14** 1632
- [30] Marin J L, Riera R and Cruz S A 1998 *J. Phys.: Condens. Matter* **10** 1349–61
- [31] Norris D J and Bawendi M G 1996 *Phys. Rev. B* **53** 16338
- [32] Allen G and Delerue C 2004 *Phys. Rev. B* **70** 245321
- [33] Kuno M, Lee J K, Dabbousi B O, Mikulec F V and Bawendi M G 1997 *J. Chem. Phys.* **106** 9889
- [34] Takagahara T and Takeda K 1992 *Phys. Rev. B* **46** 15578
- [35] Andreev A D and Lipovskii A A 1999 *Phys. Rev. B* **59** 15402
- [36] Tudury G E, Marquezini M V, Ferreira L G, Barbosa L C and Cesar C L 2000 *Phys. Rev. B* **62** 7357
- [37] Hens Z *et al* 2004 *Phys. Rev. Lett.* **92** 026808
- [38] Fernée M J, Watt A, Warner J, Cooper S, Heckenberg N and Rubinsztein-Dunlop H 2003 *Nanotechnology* **14** 991
- [39] Krauss T D, Wise F W and Tanner D B 1996 *Phys. Rev. Lett.* **76** 1376
- [40] Upadhyaya K S, Yadav M and Upadhyaya G K 2002 *Phys. Status Solidi b* **229** 1129
- [41] Guyot-Sionnest P, Wehrenburg B and Yu D 2005 *J. Chem. Phys.* **123** 074709